Can Magnetic Resonance Imaging–Derived Bone Models Be Used for Accurate Motion Measurement with Single-Plane Three-Dimensional Shape Registration?

Taka-aki Moro-oka,[1,2,3] Satoshi Hamai,[3] Hiromasa Miura,[3] Takeshi Shimoto,[4] Hidehiko Higaki,[4] Benjamin J. Fregly,[1] Yukihide Iwamoto,[3] Scott A. Banks[1,5]

[1]Department of Mechanical & Aerospace Engineering, University of Florida, 318 MAE-A, Mail Stop 116250, Gainesville, Florida 32611-6250

[2]Seimeikai Moro-oka Orthopaedic Hospital, Fukuoka, Japan

[3]Department of Orthopaedic Surgery, Graduate School of Medical Sciences, Kyushu University, Fukuoka, Japan

[4]Department of Mechanical Engineering, Faculty of Engineering, Kyushu Sangyo University, Fukuoka, Japan

[5]The BioMotion Foundation, Palm Beach, Florida

Received 30 March 2006; accepted 8 November 2006

Published online 8 February 2007 in Wiley InterScience (www.interscience.wiley.com). DOI 10.1002/jor.20355

ABSTRACT: The purpose of this study was to compare three-dimensional (3D) kinematic measurements from single-plane radiographic projections using bone models created from magnetic resonance imaging (MRI) and computed tomography (CT). MRI is attractive because there is no ionizing radiation, but geometric field distortion and poor bone contrast degrade model fidelity compared to CT. We created knee bone models of three healthy volunteers from both MRI and CT and performed three quantitative comparisons. First, differences between MRI– and CT–derived bone model surfaces were measured. Second, shape matching motion measurements were done with bone models for X-ray image sequences of a squat activity. Third, synthetic X-ray images in known poses were created and shape matching was again performed. Differences in kinematic results were quantified in terms of root mean square (RMS) error. Mean differences between CT and MRI model surfaces for the femur and tibia were −0.08 mm and −0.14 mm, respectively. There were significant differences in three of six kinematic parameters comparing matching results from MRI–derived bone models and CT–derived bone models. RMS errors for tibiofemoral poses averaged 0.74 mm for sagittal translations, 2.0 mm for mediolateral translations, and 1.4° for all rotations with MRI models. Average RMS errors were 0.53 mm for sagittal translations, 1.6 mm for mediolateral translations, and 0.54° for all rotations with the CT models. Single-plane X-ray imaging with model-based shape matching provides kinematic measurements with sufficient accuracy to assess knee motions using either MRI– or CT–derived bone models. However, extra care should be taken when using MRI–derived bone models because model inaccuracies will affect the quality of the shape matching results. © 2007 Orthopaedic Research Society. Published by Wiley Periodicals, Inc. J Orthop Res 25:867–872, 2007

Keywords: magnetic resonance imaging (MRI); image distortion; computed tomography (CT); three-dimensional kinematics; knee

INTRODUCTION

Shape matching techniques have been used for 15 years to determine knee arthroplasty motions from fluoroscopic image sequences.[1–3] Recently, these techniques have been applied for motion measurement in joints without metallic implants, where three-dimensional (3D) surface models of the bones are created from magnetic resonance imaging (MRI)[4] and computed tomography (CT).[2,5–7] However, we are unaware of any rigorous assessment of the use of MRI–derived models for the purpose of shape registration–based motion measurement. DeFrate and colleagues reported the advantages of MRI-based model creation included the ability to add cartilage to the models and to avoid radiation exposure, but they did not directly assess the accuracy of their

Correspondence to: Scott A. Banks (Telephone: 352-392-6109; Fax: 352-392-7303; E-mail: banks@ufl.edu)

shape matching technique using the MRI–derived bone models.[4,8] It is well recognized that MRI provides lower bone contrast than CT and suffers from spatial distortions which vary by scanner, scan sequence, and the object being scanned.[9–18] MRI use is limited, for example, in stereotactic surgery of the brain unless geometric distortion correction has been performed.[14,15] Similarly, shape registration–based motion measurement requires submillimeter model accuracy for many clinically relevant measurement scenarios. In contrast, CT has negligible scaling error because images are reconstructed from line-of-sight X-ray optics.[9,11,13] The purposes of this study were to compare 3D kinematics from model-based shape matching using CT– and MRI–derived bone models and to determine if MRI–derived bone models provide sufficient fidelity to provide clinically relevant measurements.

METHODS

Three healthy subjects gave informed consent to participate in this study as approved by the institutional review board. Geometric bone models of the femur and tibia/fibula were created from CT (Toshiba, Aquilion, Tochigi, Japan) and MRI (Hitachi, Airis II Comfort, 0.3 T, Tokyo, Japan) scans of one leg. CT scans used a 512×512 image matrix, a 0.35×0.35 pixel dim, and a 1.00-mm thickness spanning approximately 150 mm above and below the joint line of the knee, and 2-mm slices through the centers of the hip and ankle joints. CT scan time was 49 s. MRI scans used a 512×512 image matrix, a 0.39×0.39 pixel dim, and a 1.0-mm thickness spanning more than 80 mm above and below the joint line of the knee. The MRI protocol was 3DT1GE, RF spoiled SARGE(RSSG). MR scan time ranged from 11 to 15 min.

Exterior cortical bone edges were segmented using commercial software (SliceOmatic, Tomovision, Montreal, CA), and these point clouds were converted into polygonal surface models (Geomagic Studio, Raindrop Geomagic, Research Triangle Park, NC). Interior cortical bone edges were not included because of poor definition in the epiphyseal and metaphyseal regions.

Anatomical coordinate systems were embedded in each bone model following a combination of previous approaches.[5,19,20] The coordinate systems were first defined for the CT models. The mediolateral (x) axes of the femur and tibia/fibula were defined by fitting a cylinder to each posterior condyle of the femur. The midpoint of the cylindrical axis was defined as the origin. The proximal/distal (y) axis for the femur was defined by a line perpendicular to the cylindrical axis in the plane intersecting the femoral head center. The proximal/distal (y) axis for the shank was perpendicular to the cylindrical axis in the plane intersecting the ankle center. The anteroposterior (z) axis was formed from the cross product of the first two. Next, the MRI model was registered with the corresponding CT model in its initial reference pose to align the embedded coordinate systems in each bone model. Automated alignment software was used with a proprietary algorithm to match 3D surfaces (Geomagic Studio). Fitting results were accurate to less than 0.1 microns in length and 0.1 arc seconds (1/36,000 of a degree) in angle compared to the official reference value.

The CT models were then shortened to the same length as the MRI models. Three experiments were performed to compare the CT and MR models.

Experiment 1

Differences between MRI and CT model surfaces were measured using inspection software (Geomagic Studio).

Experiment 2

Shape matching with the CT– and MRI–derived models was performed independently, without any information from one kinematic solution affecting the kinematic solution of the other. Continuous X-ray images of a squat activity for each subject were taken using a flat panel detector [Hitachi, Clavis, Tokyo, Japan; 3 frames/s, image area size 397 (H) $\times$ 298 (V) mm, and 0.20×0.20 mm/pixel resolution]. These images were scaled to 512×512 square pixels for 3D shape registration. A Canny edge detector was used to identify bony contours. At first, bone models were aligned manually by the order of 0.27 mm for in-plane translations, 0.95 mm for out-of-plane translation, and 0.25° for rotation. Next, an automated matching algorithm, based on nonlinear least squares optimization and an image edge-to-model edge distance criteria, was used to align both sets of bone models to 22 X-ray images for each knee (Fig. 1a). The computation time for the matching algorithm was 10 to 20 s per model (Dell precision 650, Intel Xeon processor, 2.40 GHz, 1.00 GB RAM, under the Windows XP Professional edition). Differences were quantified in terms of RMS errors ($\sqrt{bias^2 + variance}$), where bias is the mean difference and variance is the square root of the standard deviation of the differences. Student's t-test ($p < 0.05$) was used to determine if the RMS errors were significantly different from zero.

Experiment 3

The original full-length CT bone models were registered to 22 X-ray images for each knee as previously described. Synthetic X-ray images (Fig. 1b) were then created by ray tracing (Rhinoceros and Flamingo, Robert McNeel & Associates, Seattle, WA) the full-length CT bone models in these 3D poses. The same automated matching algorithm was then used to align

 DOI 10.1002/jor

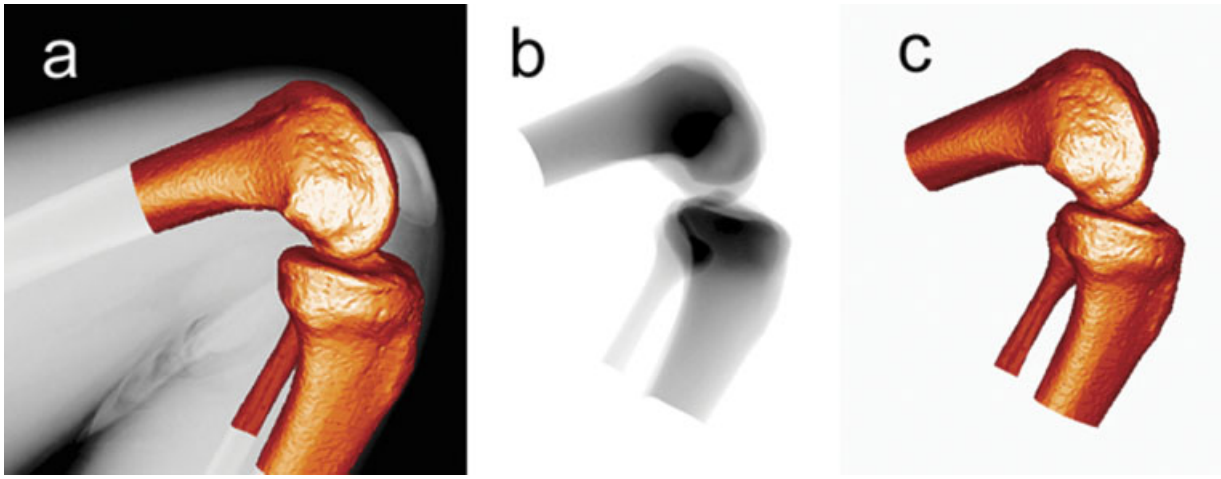

Figure 1. Matching of bone model to X-ray image (a), synthetic image generated using ray tracing (b), and matching of bone model to synthetic image (c).

shortened CT models and the MRI–derived bone models independently to the synthetic images (Fig. 1c).[1,6] RMS errors were used to compare results from the CT and MRI models. Paired t-tests ($p < 0.05$) were used to determine if there were significant differences.

RESULTS

Experiment 1

The differences between CT and MRI model surfaces (mean $\pm$ 1 SD) for the femur and tibia were -0.11 ± 0.81 mm and -0.14 ± 0.67 mm in subject 1, -0.23 ± 0.48 mm and -0.13 ± 0.48 mm in subject 2, and -0.12 ± 0.60 mm and -0.15 ± 0.77 mm in subject 3 (Fig. 2).

Experiment 2

Significant differences were found in three of six parameters (Table 1). RMS differences averaged 1.2 mm for sagittal plane translations, 2.3 mm for mediolateral translations, and 1.7° for all rotations.

Experiment 3

Average RMS errors for tibiofemoral poses were 0.74 mm for sagittal translations, 2.0 mm for mediolateral translations, and 1.4° for all rotations with MRI models. Average RMS errors were 0.53 mm for sagittal translations, 1.6 mm for mediolateral translation, and 0.54° for all rotations with the CT models (Table 2). The total amount of motion observed for each subject is shown in Table 3.

DISCUSSION

Single-plane X-ray imaging and model-based shape matching appear to provide kinematic measurements with sufficient certainty to assess

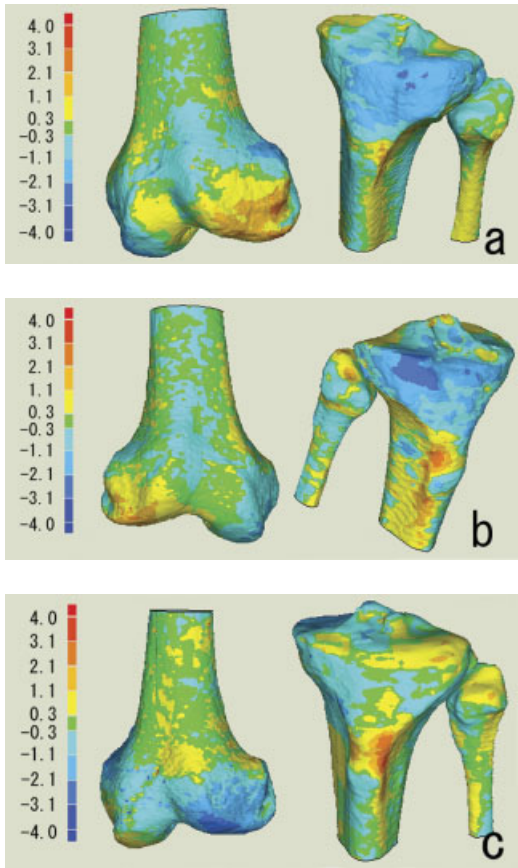

Figure 2. Three-dimensional distance measurement from CT model to MRI model (mm). (a) Subject 1, (b) subject 2, and (c) subject 3.

Table 1. Kinematic Differences When Using MRI– and CT–Derived Bone Models with In Vivo Images (RMS Differences)

Parameter	Subject 1	Subject 2	Subject 3	Average
Anterior–posterior translation (mm)	0.96	0.94	2.28	1.39
Superior–inferior translation (mm)	1.05	1.16	0.84	1.02
Medial–lateral translation (mm)	2.68	1.89	2.32	2.30*
Flexion–extension (°)	1.06	1.17	1.49	1.24*
Internal–external rotation (°)	2.35	0.92	1.54	1.60*
Varus–valgus (°)	1.82	3.42	1.71	2.32

*$p < 0.05$ from 0.

normal and pathological knee motions using either MRI– or CT–derived bone models. Nonetheless, measurement performance with CT–derived bone models was superior to measurements performed with MRI–derived models.

The results with CT–derived models improved significantly from our previous study, where only the exterior bone contours were used for shape matching.[6] Using only exterior contours resulted in average RMS errors of 1.8 mm for sagittal plane translations, 10.6 mm for mediolateral translations, and 1.1° for rotations, compared to 0.53 mm, 1.6 mm, and 0.54°, respectively, for rotations in the present study. Including internal edges for shape registration, specifically the occluded condyles of the femur and tibia and the head of the fibula, significantly improved shape-matching performance.[2] Kinematic measurement performance using single-plane fluoroscopic projections and CT–derived bone models was previously reported.[2] Komistek and colleagues reported measurement precision of 0.45 mm for sagittal plane translation and 0.66° for rotation, both comparable to our current study. Our results are also comparable to measurements using biplane radiographics and CT–derived bone models: RMS error of 0.23 mm for translations and 1.2° for rotation.[7] However, biplane techniques have more uniform errors, whereas single-plane techniques have much higher uncertainties for translations perpendicular to the image plane. No previous study exists to compare for the results with MRI–derived bone models.

Bony contours are less distinct in X-ray projections than the boundaries of metallic implants.[7] Fregly and colleagues showed that biased edge detection can be a primary factor limiting bone-model registration accuracy.[6] Thus, it is critical to adjust X-ray exposure parameters carefully to achieve good contrast around and within the joint. This is especially true for the tibia and fibula, where the fibular head tends to be obscured by the tibia and dense surrounding soft tissue, and the tibial condyles and tubercle are easily overpenetrated by the X-ray beam. Clearly defined, these bony features significantly reduce measurement uncertainty for tibial varus–valgus and internal–external rotation. Use of a high-resolution flat panel detector in the present study permitted adequate definition of these bone features. Image resolution also will affect shape-matching performance and measurement bias. Hardware and software limitations required the flat-panel detector images (1985×1490 pixels) to be resampled to 512×512 pixels for this analysis. Using higher resolution images, measurement bias could be decreased and measurement precision increased regardless of bone model source.

Table 2. Mean Kinematic Errors When Using MRI– and CT–Derived Bone Models with Synthetic Images (RMS Error)

	Subject 1		Subject 2		Subject 3		Overall		
Tibiofemoral Kinematics	MRI	CT	MRI	CT	MRI	CT	MRI	CT	*t*-Test
Anterior–posterior translation (mm)	0.60	0.44	0.84	0.56	1.19	0.97	0.88	0.66	0.024
Superior–inferior translation (mm)	0.68	0.40	0.46	0.35	0.64	0.44	0.59	0.40	0.057
Medial–lateral translation (mm)	1.54	1.96	2.69	1.34	1.69	1.47	1.97	1.59	0.54
Flexion–extension (°)	0.46	0.27	0.88	0.55	0.98	0.43	0.77	0.42	0.077
Internal–external rotation (°)	2.11	0.43	0.78	0.59	1.41	0.63	1.43	0.55	0.18
Varus–valgus (°)	2.28	0.61	1.34	0.64	1.93	0.67	1.85	0.64	0.049

 DOI 10.1002/jor

Table 3. Total Amount of Tibiofemoral Motion for 22 Images in Three Subjects (Maximum Value–Minimum Value)

Tibiofemoral Kinematics	Subject 1	Subject 2	Subject 3	Overall
Anterior–posterior translation (mm)	7.4	11.2	12.2	10.3
Superior–inferior translation (mm)	5.3	3.2	7.2	5.2
Medial–lateral translation (mm)	4.7	6.3	8.4	6.5
Flexion–extension (°)	138.4	115.8	141.5	131.9
Internal–external rotation (°)	32.76	26.48	37.70	32.31
Varus–valgus (°)	6.03	5.54	8.07	6.55

Translations were measured as the femoral coordinate origin moving with respect to the tibial coordinate origin. The amount of motion corresponds to 22 frames of data, which do not necessarily include the entire range of squat motion from full extension to full flexion.

Comparison of the bone models derived from the same subject using CT and MRI showed areas where the surfaces differed by several millimeters (Fig. 2). Several factors probably contributed to these shape differences, which result in different shape-matching performance with the CT– and MRI–derived bone models. First, the fact that different shapes are obtained from the CT and MRI scans introduces bias placing the coordinate systems in the two models. These slight offsets in coordinate system origin and orientation result directly in bias when comparing the measurements from the two models, slightly reducing the ability to isolate differences solely due to bone reconstruction fidelity. Second, bone boundaries identified in CT result directly from X-ray projections, while bone boundaries in MRI result from different physical properties. This consideration is particularly relevant at the distal femur and proximal tibia, where articular regions and ligament insertions present structures with graded properties, where the boundaries are likely to differ between CT and MRI modalities. Thus, we should expect that bone models derived from CT scans will provide superior correspondence when used for shape matching with radiographic projections.

Shape matching with in vivo images showed significant RMS differences comparing kinematics from CT– and MRI–derived bone models (Table 1). When matching the in vivo images with CT–derived bone models, no visible discrepancy was noted between the bone edges in the image and the superimposed edges of the model. With the MRI–derived models, small discrepancies between image and model edges were visible after pose optimization in most cases. Kinematics measured with synthetic X-ray projections uniformly showed less bias and better precision when CT–derived bone models were used (Table 2). Because the synthetic images were created using the CT–derived models, the accuracy and precision figures represent an absolute best-case measurement performance for similar projection geometries using the nonlinear least squares optimization method. The RMS errors figures with the MRI–derived models represent the lower boundary of measurement error one might expect using models based on different physical properties.

When using MRI to create bone models, each MRI scanner will perform differently. For this study, a 0.3 T scanner was used with a gradient echo sequence, and this provided images with sufficient bone/soft tissue contrast to identify the bone boundaries. The gradient echo sequence was used to achieve good resolution for bone segmentation,[4] but spin echo sequences are better for spatial distortion if the contrast is sufficient to detect bone boundaries.[18] Distortion increases with higher magnetic fields.[10,11,17] Higher magnetic fields increase signal intensity for better tissue resolution, but chemical shift and susceptibility artifacts also contribute to geometric distortion. Smaller magnetic fields permit narrower signal bandwidths and consequent reductions in noise. Magnetic field inhomogeneity is another source of geometric distortion that decreases with decreasing magnetic field strength.

Magnetic field inhomogeneity depends on more than field strength, being a function of materials and their spatial distribution within the object being scanned. In biological tissues, MRI signals are generated by hydrogen atoms, with water and fat content accounting for the majority of the signal. All soft tissues and cancellous bone contain a large fraction of water, so the magnetic susceptibility can be approximated by that of water. In contrast, cortical bone and air do not generate significant MRI signals. Nevertheless cortical bone can distort magnetic fields in nearby tissues that do generate

MRI signals, thereby resulting in geometric distortion near these interfaces.[16]

Finally, small motions of the patient during scanning can degrade boundary resolution and spatial integrity of the resulting models. This is of particular concern when sequences requiring long scan times are used, when the anatomy of interest is affected by normal breathing movements, and when immobilization of the area is not easily accomplished. We took great care to reduce motion artifacts while subjects were being scanned, yet it is likely small motion artifacts affected the shape of the MRI–derived bone models. Investigators should attend carefully to positioning and immobilization of subjects to produce high fidelity bone models with MRI.

Useful kinematic measurements can be obtained from single-plane fluoroscopy and shape matching using bone models derived from CT or MRI. Because the fidelity of MRI–derived bone models is degraded by a variety of technical and practical factors, shape-matching results typically will be inferior to those obtained with CT–derived bone models. However, many clinical and research situations exist in which bone model creation using MRI is highly desirable. In these cases, investigators should maintain keen awareness of the factors influencing the fidelity of bone models, and they should incorporate these technical limitations into the interpretation of their findings. Carefully done and cautiously interpreted, we should be able to expand the range of useful kinematic observations using MRI–derived bone models.

ACKNOWLEDGMENTS

No external funds were received in support of this research.

REFERENCES

1. Banks SA, Hodge WA. 1996. Accurate measurement of three-dimensional knee replacement kinematics using single-plane fluoroscopy. IEEE Trans Biomed Eng 43: 638–649.
2. Komistek RD, Dennis DA, Mahfouz M. 2003. In vivo fluoroscopic analysis of the normal human knee. Clin Orthop 69–81.
3. Yamazaki T, Watanabe T, Nakajima Y, et al. 2004. Improvement of depth position in 2-D/3-D registration of knee implants using single-plane fluoroscopy. IEEE Trans Med Imaging 23:602–612.
4. DeFrate LE, Sun H, Gill TJ, et al. 2004. In vivo tibiofemoral contact analysis using 3D MRI-based knee models. J Biomech 37:1499–1504.
5. Asano T, Akagi M, Tanaka K, et al. 2001. In vivo three-dimensional knee kinematics using a biplanar image-matching technique. Clin Orthop 157–166.
6. Fregly BJ, Rahman HA, Banks SA. 2005. Theoretical accuracy of model-based shape matching for measuring natural knee kinematics with single-plane fluoroscopy. J Biomech Eng 127:692–699.
7. You BM, Siy P, Anderst W, et al. 2001. In vivo measurement of 3-D skeletal kinematics from sequences of biplane radiographs: application to knee kinematics. IEEE Trans Med Imaging 20:514–525.
8. Li G, Wuerz TH, DeFrate LE. 2004. Feasibility of using orthogonal fluoroscopic images to measure in vivo joint kinematics. J Biomech Eng 126:314–318.
9. Doran SJ, Charles-Edwards L, Reinsberg SA, et al. 2005. A complete distortion correction for MR images: I. Gradient warp correction. Phys Med Biol 50:1343–1361.
10. Hawnaur JM, Isherwood I. 2000. MRI at midfield strength. In: Young IR editor. Methods in biomedical magnetic resonance imaging and spectroscopy. Chichester, UK; Wiley: p 39–47.
11. Hill DL, Maurer CR Jr, Studholme C, et al. 1998. Correcting scaling errors in tomographic images using a nine degree of freedom registration algorithm. J Comput Assist Tomogr 22:317–323.
12. Kaufman L, Kramer D, Carlson J, et al. 2000. Low-field whole body systems. In: Young IR editor. Methods in biomedical magnetic resonance imaging and spectroscopy. Chichester, UK; Wiley: p 30–39.
13. Langlois S, Desvignes M, Constans JM, et al. 1999. MRI geometric distortion: a simple approach to correcting the effects of non-linear gradient fields. J Magn Reson Imaging 9:821–831.
14. Maurer CR Jr, Aboutanos GB, Dawant BM, et al. 1996. Effect of geometrical distortion correction in MR on image registration accuracy. J Comput Assist Tomogr 20:666–679.
15. Moore CS, Liney GP, Beavis AW. 2004. Quality assurance of registration of CT and MRI data sets for treatment planning of radiotherapy for head and neck cancers. J Appl Clin Med Phys 5:25–35.
16. Sumanaweera T, Glover G, Song S, et al. 1994. Quantifying MRI geometric distortion in tissue. Magn Reson Med 31:40–47.
17. Vlaardingerbroek MT, Boer JAd. 1999. Magnetic resonance imaging. 2nd ed. New York: Springer; p 185–187.
18. Young IR editor. 2000. Biomedical magnetic resonance imaging and spectroscopy. Chichester, UK: Wiley.
19. Eckhoff DG, Bach JM, Spitzer VM, et al. 2005. Three-dimensional mechanics, kinematics, and morphology of the knee viewed in virtual reality. J Bone Joint Surg [Am] 87: (Suppl 2):71–80.
20. Roos PJ, Neu CP, Hull ML, et al. 2005. A new tibial coordinate system improves the precision of anterior-posterior knee laxity measurements: a cadaveric study using Roentgen stereophotogrammetric analysis. J Orthop Res 23:327–333.